HAL open science

Spectral analysis by direct and adjoint Monte Carlo methods

Vito Vitali, Florent Chevallier, Alexis Jinaphanh, Patrick Blaise, Andrea Zoia

To cite this version:

Vito Vitali, Florent Chevallier, Alexis Jinaphanh, Patrick Blaise, Andrea Zoia. Spectral analysis by direct and adjoint Monte Carlo methods. Annals of Nuclear Energy, 2020, 137, pp.107033. 10.1016/j.anucene.2019.107033 . hal-03488748

HAL Id: hal-03488748

https://hal.science/hal-03488748v1

Submitted on 21 Jul 2022

HAL is a multi-disciplinary open access archive for the deposit and dissemination of scientific research documents, whether they are published or not. The documents may come from teaching and research institutions in France or abroad, or from public or private research centers.

L'archive ouverte pluridisciplinaire **HAL**, est destinée au dépôt et à la diffusion de documents scientifiques de niveau recherche, publiés ou non, émanant des établissements d'enseignement et de recherche français ou étrangers, des laboratoires publics ou privés.

Distributed under a Creative Commons Attribution - NonCommercial 4.0 International License

Version of Record: https://www.sciencedirect.com/science/article/pii/S0306454919305353
Manuscript_b11d7417a3afb2e5cc986eb354caf475

Spectral analysis by direct and adjoint Monte Carlo methods

Vito Vitali[a], Florent Chevallier[a], Alexis Jinaphanh[a], Patrick Blaise[b], Andrea Zoia[a,*]

[a] *DEN-Service d'études des réacteurs et de mathématiques appliquées (SERMA), CEA, Université Paris-Saclay, F-91191, Gif-sur-Yvette, France*
[b] *CEA, DEN, DER, Cadarache, 13115 Saint-Paul-Lez-Durance, France*

Abstract

Time or α eigenvalues are key to several applications in reactor physics, encompassing start-up analysis and reactivity measurements. In a series of recent works, a Monte Carlo method has been proposed in order to estimate the elements of the matrices that represent the discretized formulation of the operators involved in the α-eigenvalue problem, which paves the way towards the spectral analysis of time-dependent systems (Betzler, 2014; Betzler et al., 2014, 2015, 2018). In this work, we improve the existing methods in two directions. We first show that the α-k modified power iteration scheme can be successfully applied to the estimation of the matrix elements in the direct formulation of the eigenvalue problem, which removes the bias on the fundamental eigenvalue and eigenvector of the discretized matrix, similarly to what happens for the fission matrix in the k-eigenvalue problems. Then, we show that the matrix elements for the adjoint formulation of the α eigenvalue problem can be estimated by using the Generalized Iterated Fission Probability method, which we have introduced in order to compute the fundamental adjoint α eigenfunction. We will verify the proposed algorithms and probe their convergence as a function of the size of the discretized matrices on some simplified benchmark configurations where exact reference solutions can be obtained.

Keywords: Time eigenvalues, Monte Carlo, direct, adjoint, matrix, eigenfunctions

*Corresponding author
Email address: andrea.zoia@cea.fr (Andrea Zoia)

© 2019 published by Elsevier. This manuscript is made available under the CC BY NC user license
https://creativecommons.org/licenses/by-nc/4.0/

1. Introduction

The characterization of the time behaviour of the system under analysis is key to several applications emerging in reactor physics, including pulsed neutron reactivity measurements (Pázsit and Pál, 2008; Cao and Lee, 2010; Hansen, 1985), reactor period analysis (Keepin, 1965; Zoia and Brun, 2016; Zoia et al., 2016; Nauchi, 2013), reactor start-up (Pfeiffer et al., 1974), material control and accountability in critical assemblies (Sanchez and Jaegers, 1998), accelerator-driven systems (Persson, 2008) and perturbation theory (Yamamoto and Sakamoto, 2019; Favorite, 2018; Yamamoto and Sakamoto, 2019; Jinaphanh and Zoia, 2019). The time evolution of neutron transport is governed by the Boltzmann equation, possibly coupled to the equations for the delayed neutron precursors (Bell and Glasstone, 1970). Monte Carlo simulation is considered as the gold standard for the simulation of neutron transport, in that almost no approximations are introduced, contrary to faster but approximate deterministic methods. Due to their high computational cost, Monte Carlo methods have been so far mostly devoted to the analysis of stationary systems. However, thanks to the increasing CPU power, the direct (kinetic) simulation of time-dependent transients including neutrons and precursors has become accessible and will establish itself as the reference verification tool for deterministic solvers in non-stationary regime in the near future (Sjenitzer and Hoogenboom, 2013; Faucher et al., 2018).

Beside kinetic simulations, the assessment of the time evolution of the neutron population can be usefully complemented by the spectral analysis of the Boltzmann operator (Duderstadt and Martin, 1979). This is tantamount to determining the so-called time (or α) eigenvalues and eigenmodes that stem from supposing variable separation and a time dependence of the kind $\exp(\alpha t)$ for both the neutron flux and the precursor concentrations. The eigenvalues α, carrying the units of inverse time, correspond to a set of characteristic reactor frequencies; the dominant α eigenvalue, i.e., the one having the largest real part, physically represents the inverse asymptotic reactor period, and the associated dominant eigenmode $\left\{\varphi_\alpha, c_\alpha^1, \cdots, c_\alpha^J\right\}$ represents the asymptotic distribution of neutrons and precursors (for families 1 to J) within the reactor at long times. Several Monte Carlo methods exist to determine the dominant α eigenvalue and eigenmode, encompassing the α-k modified power iteration (Brockway et al., 1985; Cullen, 2003; Zoia et al., 2015), the time-source technique (Shim et al., 2015) and root finding procedures (Hoogenboom, 2002; Nauchi, 2013; Josey, 2018). Despite some successful attempts, direct Monte Carlo simulation of higher α eigenvalues and eigenmodes has received only limited attention (Yamamoto, 2011). In this context, matrix-filling Monte Carlo methods have recently drawn much in-

terest (Betzler, 2014; Betzler et al., 2014, 2015, 2018): the underlying idea is to estimate by Monte Carlo simulation the elements of a matrix whose eigenvalues and eigenvectors converge to the true α eigenvalues and eigenmodes in the limit of a sufficiently fine discretization of the phase space (Betzler et al., 2018) [1]. This approach is very similar in spirit to the better-known fission matrix method for k-eigenvalues (Dufek and Gudowski, 2009; Carney et al., 2014). Although the α eigenvalues and eigenmodes thus estimated are generally biased because of the finite size of the matrix, this method allows obtaining a fairly accurate picture of the entire spectrum and thus grasping the time evolution of the system (Betzler et al., 2014, 2015), even for complex three-dimensional configurations (Betzler, 2014; Betzler et al., 2018). Moreover, once the α spectrum and the associated eigenvectors have been determined from the matrix, the full time-dependent evolution of the neutron and precursor populations can also be reconstructed, at least in principle, by using the direct and adjoint matrices (Betzler et al., 2018).

The proposed matrix-filling Monte Carlo method based on a transition rate method related to the adjoint formulation of the α eigenvalue equation [2] suffers however from two approximations: the first is due to the fact that the exact adjoint formulation is in practice replaced by a forward formulation, in order to avoid the explicit simulation of backward random walks (Betzler, 2014; Betzler et al., 2018). The second is due to the fact that the matrix elements are estimated and filled in the course of a k-eigenvalue or c-eigenvalue Monte Carlo calculation, which induces a systematic bias even on the fundamental eigenvalue and eigenvector (Betzler, 2014; Betzler et al., 2018). Although both approximations vanish in the limit of a sufficiently fine discretization of the phase space, for realistic systems this might require very large matrix sizes, entailing severe memory footprint issues: contrary to the fission matrix, where only a spatial discretization is required, the matrix associated to α-eigenvalue problems demands a full discretization of the phase space, including space, direction and energy (Betzler, 2014).

In this work we will improve the estimation of the matrix elements for α eigenvalue problems in two directions. First, we will show that it is convenient to fill the elements of the matrix by using the α-k modified power itera-

[1] We remark in passing that an independent approach has been recently proposed for α eigenvalue problems, based on a time-discretization of the fission matrix (Josey and Brown, 2019). However, it appears that such method allows only determining the eigenvalues but not the eigenvectors.

[2] This is required since the authors formally work with the propagator of the underlying random walks, which is by construction associated to the adjoint evolution operators (Betzler, 2014; Betzler et al., 2018).

tion: this approach allows natively preserving the fundamental eigenvalue and eigenvector, which will be computed exactly [3]. Second, we will show that it is actually possible to compute the matrix elements corresponding to the adjoint α eigenvalue equations by using the Generalized Iterated Fission Probability (IFP) method that we have recently introduced (Terranova et al., 2017): the obtained adjoint-weighted matrix will correspondingly preserve the fundamental (adjoint) eigenvalue and eigenvector, as opposed to building the adjoint operator matrix by transposing the direct operator matrix.

This paper is organized as follows: in Sec. 2 we will briefly recall the direct and adjoint formulation of the α eigenvalue problem. In Sec. 3 we will detail the Monte Carlo algorithms that allow estimating the matrix elements corresponding to the discretized formulation of the operators appearing in the α eigenvalue equations, for both the direct and adjoint problems. Numerical examples for the verification of the proposed algorithms will be discussed in Sec. 4: for this purpose we will consider some simplified benchmark configurations where exact reference solutions can be obtained. A discussion concerning the obtained matrix operators and their application to realistic configurations is presented in Sec. 5. Conclusions will be finally drawn in Sec. 6.

2. The α eigenvalue equations

Time eigenvalue equations are obtained from the Boltzmann equation for the time-dependent neutron flux $\varphi(\mathbf{r},\mathbf{\Omega},E,t)$ and from the equations for the time-dependent delayed neutron precursors $c_j(\mathbf{r},t)$ by postulating variable separation of the kind $\varphi(\mathbf{r},\mathbf{\Omega},E,t)=\varphi_\alpha(\mathbf{r},\mathbf{\Omega},E)\exp(\alpha t)$ and $c_j(\mathbf{r},t)=c^j_\alpha(\mathbf{r})\exp(\alpha t)$ (Bell and Glasstone, 1970). This leads to the system of eigenvalue equations

$$\begin{aligned}
&\frac{\alpha}{v}\varphi_\alpha+\mathcal{L}\varphi_\alpha=\mathcal{F}_p\varphi_\alpha+\sum_j\frac{\chi^j_d(E)}{4\pi}c^{\alpha,j}\\
&\alpha c_{\alpha,j}=\mathcal{F}_{d,j}\varphi_\alpha-\lambda_j c_{\alpha,j},
\end{aligned}\tag{1}$$

$j=1,\cdots,J$. Here $\mathcal{L}$ denotes the net disappearance operator

$$\mathcal{L}=\mathbf{\Omega}\cdot\nabla+\Sigma_t-\int\int d\mathbf{\Omega}'dE'\Sigma_s(\mathbf{r},\mathbf{\Omega}',E'\to\mathbf{\Omega},E),\tag{2}$$

[3]The same choice appears to have been independently proposed by (Variansyah et al., 2019).

$\mathcal{F}_p$ the prompt fission operator

$$\mathcal{F}_p = \frac{\chi_p(\mathbf{r}, E)}{4\pi} \int \int d\mathbf{\Omega}' dE' \nu_p(E') \Sigma_f(\mathbf{r}, E'), \tag{3}$$

and $\mathcal{F}_{d,j}$ the delayed fission operator associated to precursor family j

$$\mathcal{F}_{d,j} = \int \int d\mathbf{\Omega}' dE' \nu_{d,j}(E') \Sigma_f(\mathbf{r}, E'), \tag{4}$$

where Σ_x, χ and ν stand respectively for the macroscopic cross section of reaction x, fission spectrum and multiplicity, and λ_j are the precursor decay constants for family j. In order to keep notation to a minimum, we consider a single fissile nucleus. The system in Eqs. (1) can be rewritten in a suggestive matrix form as

$$\mathcal{A}\psi_\alpha = \alpha \mathcal{B} \psi_\alpha \tag{5}$$

for the generalized eigenfunction vector $\psi_\alpha = \{\varphi_\alpha, c_{\alpha,1}, \cdots, c_{\alpha,J}\}^T$, where we have defined the matrix operators

$$\mathcal{A} = \begin{pmatrix} \mathcal{F}_p - \mathcal{L} & \lambda_1 \frac{\chi_{d,1}(E)}{4\pi} & \cdots & \lambda_J \frac{\chi_{d,J}(E)}{4\pi} \\ \mathcal{F}_{d,1} & -\lambda_1 & \cdots & 0 \\ \vdots & \vdots & \ddots & \vdots \\ \mathcal{F}_{d,J} & 0 & \cdots & -\lambda_J \end{pmatrix} \tag{6}$$

and

$$\mathcal{B} = \begin{pmatrix} \frac{1}{v} & 0 & \cdots & 0 \\ 0 & 1 & \cdots & 0 \\ \vdots & \vdots & \ddots & \vdots \\ 0 & 0 & \cdots & 1 \end{pmatrix} \tag{7}$$

The spectral properties of the eigenvalue system in Eq. (5) are highly non-trivial and have attracted intensive research efforts. For a review of the prompt case (i.e., when the precursors contributions are neglected), see, e.g., (Larsen and Zweifel, 1974); the general problem including precursors has received comparatively less attention (Kaper, 1967). The conditions for the well-posedness of Eqs. (5) have been extensively analyzed (Larsen and Zweifel, 1974; Duderstadt and Martin, 1979). Under mild assumptions, a dominant discrete eigenvalue α_0 exists, which is simple, real, larger than the real parts of all the other α, and whose associated eigenfunction is non-negative (Larsen and Zweifel, 1974). This ensures that, after a transient, the neutron and precursor population will grow or decay in time

as $\propto e^{\alpha_0 t}$. Due to the symmetrical nature of the involved operators, the complex eigenvalues α (if any) come in conjugate pairs and are typically associated to oscillatory modes (Larsen and Zweifel, 1974).

The equations adjoint to Eqs. (1) are obtained from the adjoint Boltzmann equation for the time-dependent adjoint neutron flux $\varphi^\dagger(\mathbf{r},\mathbf{\Omega},E,t)$ and from the equations for the time-dependent adjoint precursor concentrations $c_j^\dagger(\mathbf{r},t)$ by postulating again variable separation of the kind $\varphi^\dagger(\mathbf{r},\mathbf{\Omega},E,t)=\varphi_\alpha^\dagger(\mathbf{r},\mathbf{\Omega},E)\exp(-\alpha^\dagger t)$ and $c_j^\dagger(\mathbf{r},t)=c_{\alpha,j}^\dagger(\mathbf{r})\exp(-\alpha^\dagger t)$ (Bell and Glasstone, 1970). This leads to the system

$$\begin{aligned}
&\frac{\alpha^\dagger}{v}\varphi_\alpha^\dagger+\mathcal{L}^\dagger\varphi_\alpha^\dagger=\mathcal{F}_p^\dagger\varphi_\alpha+\sum_j \nu_{d,j}(E)\Sigma_f(\mathbf{r},E)c_{\alpha,j}^\dagger\\
&\alpha^\dagger c_{\alpha,j}^\dagger=\lambda_j\int\int d\mathbf{\Omega}'dE'\frac{\chi_{d,j}(E')}{4\pi}\varphi_\alpha^\dagger(\mathbf{r},\mathbf{\Omega}',E')-\lambda_j c_{\alpha,j},
\end{aligned}\tag{8}$$

$j=1,\cdots,J$. Here $\mathcal{L}^\dagger$ denotes the adjoint net disappearance operator

$$\mathcal{L}^\dagger=-\mathbf{\Omega}\cdot\nabla+\Sigma_t-\int\int d\mathbf{\Omega}'dE'\Sigma_s(\mathbf{r},\mathbf{\Omega},E\to\mathbf{\Omega}',E')\tag{9}$$

and $\mathcal{F}_p^\dagger$ the adjoint prompt fission operator

$$\mathcal{F}_p^\dagger=\nu_p(E)\Sigma_f(\mathbf{r},E)\int\int d\mathbf{\Omega}'dE'\frac{\chi_p(\mathbf{r},E')}{4\pi}.\tag{10}$$

The system in Eqs. (8) can be again rewritten in matrix form as

$$\mathcal{A}^\dagger\psi_\alpha^\dagger=\alpha^\dagger\mathcal{B}^\dagger\psi_\alpha^\dagger\tag{11}$$

for the generalized adjoint eigenfunction vector $\psi_\alpha^\dagger=\left\{\varphi_\alpha^\dagger,c_{\alpha,1}^\dagger,\cdots,c_{\alpha,J}^\dagger\right\}^T$, where we have defined the matrix operators

$$\mathcal{A}^\dagger=\begin{pmatrix}
\mathcal{F}_p^\dagger-\mathcal{L}^\dagger & \nu_{d,1}(E)\Sigma_f(\mathbf{r},E) & \cdots & \nu_{d,J}(E)\Sigma_f(\mathbf{r},E)\\
\lambda_1\int\int d\mathbf{\Omega}'dE'\frac{\chi_{d,1}(E')}{4\pi} & -\lambda_1 & \cdots & 0\\
\vdots & \vdots & \ddots & \vdots\\
\lambda_J\int\int d\mathbf{\Omega}'dE'\frac{\chi_{d,J}(E')}{4\pi} & 0 & \cdots & -\lambda_J
\end{pmatrix}\tag{12}$$

and $\mathcal{B}^\dagger=\mathcal{B}$. The adjoint and forward eigenvalue spectra are the complex conjugates of each other, i.e., coincide on the complex plane, and the eigenmodes satisfy a bi-orthogonality condition (Bell and Glasstone, 1970).

For given reactor configuration and external source, the full time-dependent solution $\psi = \{\varphi, c_1 \cdots, c_J\}^T$ can be expanded in terms of the α eigenfunctions as

$$\psi(\mathbf{r}, \mathbf{\Omega}, E, t) = \sum_i^I w_i(t)\psi_{\alpha_i}(\mathbf{r}, \mathbf{\Omega}, E) + \zeta(\mathbf{r}, \mathbf{\Omega}, E, t), \tag{13}$$

where ζ is a residual non-separable function stemming from the continuum portion of the α spectrum (if any) and I is the total number of eigenvalues α_i associated to Eqs. (5) (Bell and Glasstone, 1970; Duderstadt and Martin, 1979). The coefficients w_i of the expansion satisfy the differential equations

$$\frac{dw_i(t)}{dt} = \alpha_i w_i(t) + \frac{\langle \varphi^\dagger_{\alpha_i}, Q\rangle}{\langle \varphi^\dagger_{\alpha_i}, \frac{1}{v}\varphi_{\alpha_i}\rangle + \sum_j \langle c^\dagger_{\alpha_i,j}, c_{\alpha_i,j}\rangle}, \tag{14}$$

involving the adjoint eigenfunctions and the external source Q. The brackets denote integration over all phase space variables.

3. Monte Carlo estimators for the operators

In order to derive a numerically tractable formulation of the systems in Eqs. (5) and (11), we would like to replace the operators by matrices whose elements can be explicitly computed (Betzler et al., 2018). For this purpose, it is convenient to discretize the phase space over elements of the kind $\int_{V_n} d\mathbf{r} \int_{\Omega_m} d\mathbf{\Omega} \int_{E_g} dE$, where V_n, Ω_m and E_g denote space, angle and energy intervals, respectively. The idea is then to approximate any generic operator $\mathcal{H}$ appearing in Eqs. (5) and (11) by its average over the phase space element n, m, g: this defines the matrix elements

$$H_{n,m,g} = \langle \mathcal{H} \rangle_{n,m,g} \simeq \frac{\langle \mathcal{H} f \rangle_{n,m,g}}{\langle f \rangle_{n,m,g}}, \tag{15}$$

for an arbitrary weighting function f. Consequently, the eigenvalue problem in Eq. (5) is replaced by the matrix formulation

$$A\Psi_\alpha = \alpha B \Psi_\alpha \tag{16}$$

and the adjoint problem in Eq. (11) is replaced by

$$A^\dagger \Psi^\dagger_\alpha = \alpha B^\dagger \Psi^\dagger_\alpha. \tag{17}$$

Once the matrix elements have been estimated, the spectrum and the eigenvectors can be extracted by using standard linear algebra libraries (Betzler, 2014),

similarly to what is done for the fission matrices for k-eigenvalue problems (Carney et al., 2014). In the limit of a sufficiently fine discretization of the space, angle and energy intervals, $A, B \to \mathcal{A}, \mathcal{B}$ and $A^\dagger \to \mathcal{A}^\dagger$, so that the spectrum and the eigenvectors of the matrices converge to those of the exact formulation. The accuracy of the introduced approximation and the rate of convergence depend on the choice of the weighting function. We are thus left with two constraints: the matrix elements $H_{n,m,g}$ must correspond to scores that can be practically estimated by Monte Carlo methods, and the weighting function must be chosen so to minimize the discretization bias.

3.1. Estimating the direct matrix elements

In order to fill the elements of the (direct) fission matrix corresponding to k-eigenvalue problems, the natural choice is to use the fundamental k-eigenmode, which can be estimated by the regular power iteration method in Monte Carlo criticality calculations (Carney et al., 2014). This approach preserves the fundamental eigenvalue and eigenvector that can be computed from the resulting matrix, in the sense that they are unbiased independently of the size of the discretization intervals [4].

By analogy, and in view of obtaining a similar unbiased estimate of the fundamental eigenpair, it seems reasonable to choose the fundamental α-eigenmode as a weighting function for the forward eigenvalue problem in Eq. (5). The fundamental eigen-pair $\{\alpha, \psi_\alpha\}$ can be determined by applying the Monte Carlo implementation of the α-k power iteration [5], which was originally proposed for prompt decay constants (Brockway et al., 1985) and then extended to the general case with neutrons and precursors (Hoogenboom, 2002; Nauchi, 2013; Zoia et al., 2015). The idea is to iteratively seek the dominant α value that makes Eqs. (1) exactly critical with respect to a fictitious k-eigenvalue applied to the production terms on the right hand side. For positive α, the term α/v on the left hand side is interpreted as an additional capture cross section in the modified power iteration (Brockway et al., 1985; Cullen, 2003). For negative α, α/v is usually moved to the right hand side of the equation and interpreted as an additional production term (Brockway et al., 1985; Cullen, 2003). However, the

[4] This property however does not carry over to higher eigenvalues and eigenvectors of the direct fission matrix, nor to the fundamental (and higher) eigenmode of the transposed fission matrix (Carney et al., 2014).

[5] As mentioned, a few other methods exist to estimate $\{\alpha, \psi_\alpha\}$, each with distinct merits and drawbacks (Zoia et al., 2015; Nauchi, 2013; Shim et al., 2015; Josey, 2018). Here we have chosen the α-k method, which is relatively straightforward and can be conveniently adapted to adjoint calculations, independently of the sign of the system reactivity (Terranova et al., 2017).

standard implementation of this algorithm has been shown to be numerically unstable, possibly leading to abnormal termination (Hill, 1983). An improved α-k algorithm has been proposed by introducing a copy operator with associated cross section $-\eta\alpha/v$, with $\eta > 0$ (Zoia et al., 2014, 2015): this overcomes the limitations for the case of negative α by preserving the balance between destructions and productions (Mancusi and Zoia, 2018). Finally, the term $\lambda_j/(\lambda_j+\alpha)$ acts as a positive weight multiplier for the delayed neutrons (the dominant eigenvalue must satisfy $\alpha > -\min_j[\lambda_j]$). For a detailed description of the algorithm, we refer the reader to (Zoia et al., 2015).

Suppose now that we partition the phase space into N space intervals, M angle intervals and G energy intervals. The method proposed in this work for the direct matrices closely follows the strategy of (Betzler et al., 2018), except for the choice of φ_α and $c_{\alpha,j}$ as the weighting functions. The corresponding matrix elements will be thus filled by using the following Monte Carlo estimators. For the speed matrix, the only non-trivial terms are of the kind $\langle v^{-1}\varphi_\alpha\rangle_{n,m,g}$, which correspond to the average time spent by a neutron in the interval n,m,g during the cycles of the α-k power iteration. For the total collision operator we have $\langle\Sigma_t\varphi_\alpha\rangle_{n,m,g}$, which can be estimated at each collision event. For the scattering, prompt and delayed fission operators we have the matrix elements

$$\langle\langle\Sigma_s(\mathbf{r},\mathbf{\Omega}',E'\to\mathbf{\Omega},E)\varphi_\alpha(\mathbf{r},\mathbf{\Omega}',E')\rangle_{m',g'}\rangle_{n,m,g}, \tag{18}$$

$$\langle\frac{\chi_p(\mathbf{r},E)}{4\pi}\langle\nu_p(E')\Sigma_f(\mathbf{r},E')\varphi_\alpha(\mathbf{r},\mathbf{\Omega}',E')\rangle_{m',g'}\rangle_{n,m,g}, \tag{19}$$

and

$$\langle\langle\nu_{d,j}(E')\Sigma_f(\mathbf{r},E')\varphi_\alpha(\mathbf{r},\mathbf{\Omega}',E')\rangle_{m',g'}\rangle_{n}, \tag{20}$$

respectively, which can be again computed at collision events. The leakage term is first transformed by applying the Gauss theorem, and reads

$$\langle\mathbf{\Omega}\cdot\nabla\varphi_\alpha(\mathbf{r},\mathbf{\Omega},E)\rangle_{n,m,g} = \langle\int_{S_n} d\mathbf{r}'\mathbf{\Omega}\cdot\mathbf{n}\varphi_\alpha(\mathbf{r}',\mathbf{\Omega},E)\rangle_{m,g}, \tag{21}$$

where S_n is the surface enclosing the space element n and $\mathbf{n}$ is the normal to the surface. This term can be estimated by computing the current of neutrons streaming in and out the surfaces of the space element n, projected over the flight direction $\mathbf{\Omega}$ (Betzler, 2014).

As for the terms that must be weighted by the precursor concentrations, observe that $c_{\alpha,j}$ can be transformed into terms weighted by the neutron flux φ_α by

using

$$c_{\alpha,j} = \frac{1}{\alpha+\lambda_j}\mathcal{F}_{d,j}\varphi_\alpha \tag{22}$$

from Eqs. (1) and noting that α is known at each cycle of the α-k power iteration after convergence has been achieved. We have thus the matrix elements

$$\langle \frac{\lambda_j}{\alpha+\lambda_j}\frac{\chi_{d,j}(\mathbf{r},E)}{4\pi}\langle \nu_{d,j}(E')\Sigma_f(\mathbf{r},E')\varphi_\alpha(\mathbf{r},\mathbf{\Omega}',E')\rangle_{m',g'}\rangle_n, \tag{23}$$

which have the same structure as those of the prompt fission operator.

Finally, the denominators needed to normalize the matrix elements can be computed by estimating $\langle\varphi_\alpha\rangle_{n,m,g}$ and $\langle c_{\alpha,j}\rangle_n$.

When including the precursor contributions, the total matrix operator size is $(NMG+N_fJ)^2$, where $N_f \leq N$ is the number of fissile regions for which the precursor contributions must be assigned. Mainly due to the structure of the gradient operator and of the diagonal matrix associated to the precursor decay constants (Betzler, 2014), the matrix operator is however considerably sparse. Assuming a Cartesian grid for the space coordinates, with N_x, N_y and N_z components along each axis ($N = N_x \times N_y \times N_z$), the maximum number of non-null matrix entries is

$$\begin{aligned} &MG\Big[NMG+N_xN_y(N_z-1)+N_yN_z(N_x-1)+N_xN_z(N_y-1)\Big]+N_fJ \\ &\ll (NMG+N_fJ)^2, \end{aligned} \tag{24}$$

which is an important issue when considering real-world applications.

3.2. Estimating the adjoint matrix elements

Once the discretized matrix A has been filled, the adjoint matrix $A^\dagger$ can be in principle obtained by transposing A (Betzler et al., 2018), similarly as done for the adjoint fission matrix in k-eigenvalue problems (Carney et al., 2014). This approach would preserve the spectrum [6] (and in particular the fundamental eigenvalue) but would also induce a bias on the fundamental adjoint eigenvector, since the matrix elements would have been weighted by the forward fundamental eigenmode φ_α instead of the adjoint fundamental eigenmode $\varphi_\alpha^\dagger$ (Betzler et al., 2018). This issue is entirely analogous to what happens for the adjoint fission

[6] This consideration follows from the spectrum of a transposed real matrix being identical to the spectrum of the original matrix.

matrix in k-eigenvalue problems (Carney et al., 2014). Although this bias vanishes in the limit of sufficiently large matrices, for the sake of numerical accuracy (and in view of reducing the memory footprint) it would be convenient to estimate the adjoint matrix elements directly.

In a recent work, a generalization of the Iterated Fission Probability (IFP) method has been proposed in order to evaluate $\varphi_\alpha^\dagger$ (and more generally bi-linear forms requiring both φ_α and $\varphi_\alpha^\dagger$) by relating the fundamental adjoint eigenfunction to the neutron importance I_α (Terranova et al., 2017), similarly to what is done for the regular k-eigenvalue IFP formulation (Nauchi and Kameyama, 2010; Kiedrowski et al., 2011). The Generalized IFP method provides estimates of the neutron importance I_α in α-eigenvalue problems by recording the descendants after a given number of latent generations for an ancestor neutron starting with coordinates $\mathbf{r}, \mathbf{\Omega}, E$. In practice, I_α is estimated by using a fixed-source calculation, where neutrons are followed over the latent generations. The fundamental α eigenvalue is assumed to be known before running the calculation. For $\alpha > 0$, the additional term α/v acts as a sterile capture, as mentioned above: neutrons can contribute to I_α only being promoted to the next latent generation by prompt and delayed fission (in this latter case, their weight is assigned a correction factor $\lambda_j/(\lambda_j+\alpha)$). For $\alpha < 0$, neutrons can contribute to I_α also via the copy operator with associated cross section $-\eta\alpha/v$. The corresponding importance $I_\alpha \propto \varphi_\alpha^\dagger$ of the ancestor neutron is estimated at the end of the latent generations as

$$\langle \varphi_\alpha^\dagger Q \rangle \propto \sum_i \pi_i, \tag{25}$$

where π_i is the corresponding statistical weight of the descendants collected at the end of the Generalized IFP cycle for the neutrons initially sampled from a fixed source Q, the sum being extended over the ancestors (Terranova et al., 2017).

For the direct matrices, the α-k power iteration ensures that particles are sampled according to the fundamental eigenmode distribution and matrix elements can be constructed as regular reaction rates, as detailed above. For adjoint matrix elements, on the contrary, the idea is to carefully select a source distribution Q such that Eq. (25) yields the desired adjoint matrix element. Indeed, the adjoint matrix elements illustrated in the previous sections can all be written in the form of a scalar product involving a 'source' weighted by the fundamental adjoint mode, which can be thus estimated by computing the neutron importance function by the Generalized IFP method. Bearing in mind these considerations, two cases are encountered: if the source for the matrix element is a probability density function (e.g., a fission spectrum), this probability density

can be straightforwardly used so as to sample the initial coordinates of the neutron whose importance must be assessed. If the source for the matrix does not lend itself to be interpreted as a probability density function (e.g., the total cross section appearing in the adjoint collision matrix $\langle \Sigma_t \varphi^\dagger \rangle_{nmg}$), then an artificial uniform coordinate is sampled in the selected bin corresponding to the matrix element, and the source appearing in the expression of the matrix element will be used as a final weighting factor for the obtained importance following from the sampled neutron. For the discretized operators, a uniform meshing of the phase space is preferred, since the effect of the distribution will vanish when normalizing by the bin-integrated adjoint flux $\langle \varphi^\dagger \rangle_{nmg}$.

Similarly as in the direct case, the non-trivial part of the speed matrix is represented by a diagonal matrix with element $\langle \frac{1}{v} \varphi^\dagger \rangle_{nmg}$. The scattering

$$\langle \langle \Sigma_s(\mathbf{r}, \mathbf{\Omega}, E \to \mathbf{\Omega}', E') \varphi_\alpha^\dagger(\mathbf{r}, \mathbf{\Omega}', E') \rangle_{m',g'} \rangle_{n,m,g}, \tag{26}$$

and fission

$$\langle \nu_p(E) \Sigma_f(\mathbf{r}, E) \langle \frac{\chi_p(\mathbf{r}, E')}{4\pi} \varphi_\alpha^\dagger(\mathbf{r}, \mathbf{\Omega}', E') \rangle_{m',g'} \rangle_{n,m,g}, \tag{27}$$

matrix elements are obtained by uniformly sampling the incident energy and direction, then sampling the scattering (respectively fission) spectrum and finally computing the adjoint flux by using the Generalized IFP scheme. It is worth noting that the normalization of these elements is performed with respect to the integrated adjoint flux $\langle \varphi_\alpha^\dagger \rangle_{n,m,g}$, which requires a separate calculation, as $\langle \varphi_\alpha^\dagger \rangle_{n,m,g}$ stems from a source different from those needed for Eqs. (26) and (27).

The adjoint leakage matrix is expressed by applying again the Gauss theorem in order to convert the volume integration into a surface integration over the boundaries of the spatial bin. This leads to

$$\langle -\mathbf{\Omega} \cdot \nabla \varphi_\alpha^\dagger(\mathbf{r}, \mathbf{\Omega}, E) \rangle_{n,m,g} = -\langle \int_{S_n} d\mathbf{r}' \mathbf{\Omega} \cdot \mathbf{n} \varphi_\alpha^\dagger(\mathbf{r}', \mathbf{\Omega}, E) \rangle_{m,g}. \tag{28}$$

The expression in Eq. (28) can be given a probabilistic interpretation: the integral over the surface means that the starting points for the neutron ancestors must be taken uniformly over the boundaries of the spatial bins. The angular factor $\mathbf{\Omega} \cdot \mathbf{n}$, where $\mathbf{n}$ is the normal vector of the surface S_n, implies that the starting direction for the ancestors must be sampled by respecting an isotropic incident flux on S_n [7]. This completely defines the source for the importance calculation of the leakage term.

[7] The term $\cos\theta_0 = \mathbf{\Omega}_0 \cdot \mathbf{n}$ implies that in polar coordinates ancestors starting on the surface must enter the domain with $\theta_0 = \arcsin(2\xi - 1)$ in two dimensions and $\theta_0 = 1/2 \arccos(1 - 2\xi)$ in three dimensions, ξ being uniformly distributed in $(0, 1]$ (Zoia et al., 2012).

The adjoint precursor concentrations $\langle c_j^\dagger \rangle_n$ can be estimated by resorting again to the adjoint neutron flux, using

$$c_{\alpha,j}^\dagger = \frac{\lambda_j}{\alpha+\lambda_j} \int\int d\mathbf{\Omega}' dE' \frac{\chi_{d,j}(E')}{4\pi} \varphi_\alpha^\dagger(\mathbf{r},\mathbf{\Omega}',E'). \tag{29}$$

This leads to the following matrix elements

$$\frac{\lambda_j}{\alpha+\lambda_j} \langle \nu_{d,j}(E)\Sigma_f(\mathbf{r},E)\langle \frac{\chi_{d,j}(\mathbf{r},E')}{4\pi} \varphi_\alpha^\dagger(\mathbf{r},\mathbf{\Omega}',E')\rangle_{m',g'}\rangle_n, \tag{30}$$

which have the same structure as those of the adjoint prompt fission operator.

4. Numerical simulations

In order to assess the impact of using the α-k power iteration and the Generalized IFP method in order to fill the matrix elements of the direct and adjoint α matrices, respectively, we have selected some simplified benchmark configurations that allow more easily probing the proposed methods by comparing the obtained results to reference solutions.

4.1. The rod model

The rod model is among the simplest space- and direction-dependent transport problems: neutrons move at constant speed v along a line, where only two directions of flight are allowed, namely forward ($\mathbf{\Omega} = +$) and backward ($\mathbf{\Omega} = -$) (Wing, 1962). We will furthermore assume that scattering and fission are isotropic. Defining $\varphi_\alpha(x,\pm)$ the angular flux in the positive and negative direction, the α eigenvalue equations read

$$\pm\frac{\partial}{\partial x}\varphi_\alpha(x,\pm) + \left[\frac{\alpha}{v} + \Sigma_t\right]\varphi_\alpha(x,\pm) = \frac{\zeta_\alpha}{2}\varphi_\alpha(x), \tag{31}$$

where we have defined $\varphi_\alpha(x) = \varphi_\alpha(x,+) + \varphi_\alpha(x,-)$, and

$$\zeta_\alpha = \Sigma_s + \nu_p\Sigma_f + \sum_{j=1}^{J} \frac{\lambda_j}{\lambda_j+\alpha}\nu_{d,j}\Sigma_f. \tag{32}$$

Let us consider a segment $[0,L]$, with leakage boundary conditions $\varphi_\alpha(0,+) = 0$ and $\varphi_\alpha(L,-) = 0$. It is possible to derive an equation for $\varphi_\alpha(x)$ alone, namely,

$$-D_\alpha \frac{\partial^2}{\partial x^2}\varphi_\alpha(x) = \frac{\zeta_\alpha D_\alpha - 1}{D_\alpha}\varphi_\alpha(x), \tag{33}$$

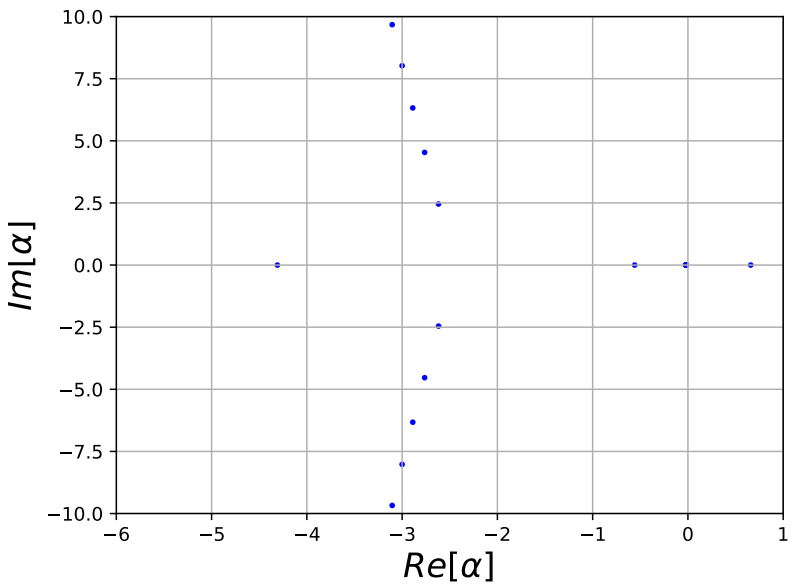

Figure 1: The spectrum of the rod model with neutrons and two precursor families, as from Eq. (37). Model parameters are the following: $L = 2$, $v = 1$, $\Sigma_s = 2$, $\Sigma_c = 1$, $\Sigma_f = 3$, $\nu = 2$, $\beta = 0.006$, $\nu_p = (1-\beta)\nu$, $\lambda_1 = 0.02$, $\beta_1 = 0.004$, $\nu_{d,1} = \beta_1\nu$, $\lambda_2 = 0.4$, $\beta_1 = 0.002$, $\nu_{d,2} = \beta_2\nu$.

with Robin boundary conditions $\varphi_\alpha(0) - D_\alpha\partial\varphi_\alpha(0) = 0$ and $\varphi_\alpha(L) + D_\alpha\partial\varphi_\alpha(L) = 0$, and

$$D_\alpha = \frac{1}{\Sigma_t + \frac{\alpha}{v}}. \tag{34}$$

The general solutions of Eq. (33) can be explicitly derived (Grebenkov and Nguyen, 2013), and read

$$\varphi_\alpha(x) = \sqrt{\zeta_\alpha D_\alpha - 1}\cos\left(\frac{\sqrt{\zeta_\alpha D_\alpha - 1}}{D_\alpha}x\right) + \sin\left(\frac{\sqrt{\zeta_\alpha D_\alpha - 1}}{D_\alpha}x\right), \tag{35}$$

from which we can obtain the angular flux $\varphi_\alpha(x,\pm)$ and the precursor concentration

$$c_{\alpha,j} = \frac{1}{\lambda_j + \alpha}\nu_{d,j}\Sigma_f\varphi_\alpha(x) \tag{36}$$

by observing that the particle current $P_\alpha(x) = \varphi_\alpha(x,+) - \varphi_\alpha(x,-)$ satisfies $P_\alpha(x) = -D_\alpha\partial_x\varphi_\alpha(x)$. The adjoint eigenmodes satisfy the relation $\varphi^\dagger_\alpha(x,\pm) = \varphi_\alpha(x,\mp)$.

v	Σ_c	Σ_f	Σ_s	ν_p	L
10	1	0.1	1	2.5	10

Table 1: Parameter values for the rod model.

weighting function	α_0	α_1	$\alpha_{2,3}$
exact	-0.91112104	-1.1402085	-1.5903273 ± 0.46007369i
α-k	-0.91112673	-1.1408138	-1.5924502± 0.45965067i
Generalized IFP	-0.91102399	-1.1410052	-1.5923255± 0.45948174i
k	-0.91103714	-1.1404864	-1.5923147 ± 0.45890215i
fixed-source	-0.91135365	-1.1407772	-1.5927331 ± 0.45864404i

Table 2: Rod model. Comparison of the α eigenvalues obtained from the matrices filled with the method shown in the first column, for $N = 1024$ spatial meshes.

The α eigenvalues stem from the dispersion law (Zoia et al., 2015)

$$\Lambda(\alpha) = 2\sqrt{\zeta_\alpha D_\alpha - 1}\cos\left(\frac{\sqrt{\zeta_\alpha D_\alpha - 1}}{D_\alpha}L\right) - \zeta_\alpha D_\alpha \cos\left(\frac{\sqrt{\zeta_\alpha D_\alpha - 1}}{D_\alpha}L\right) = 0, \quad (37)$$

which is obtained by imposing the boundary conditions on the general solutions in Eq. (35). The zeros of Eq. (37) form the discrete spectrum of the α eigenvalues for the rod model. When the precursor contributions are neglected, $\Lambda(\alpha)$ yields a finite number of real eigenvalues, plus a countable infinity of complex eigenvalues associated to oscillating modes (Montagnini and Pierpaoli, 1971); when precursors are taken into account, J additional sets of denumerable real eigenvalues are introduced by the J singularities at $\alpha = -\lambda_j$, accumulating at the right of each $-\lambda_j$. For an illustration, see Fig. 1. Equation (37) can be solved numerically by any root tracking algorithm: the direct and adjoint modes can be then obtained based on Eq. (35). As such, the rod model is ideally suited to verify the accuracy of the modal analysis methods described above.

4.1.1. Analysis of the direct eigenpairs

We begin our analysis by considering the case of direct eigenvalues and eigenfunctions. The physical parameters for the rod model are given in Tab. 1. For this example, we have chosen a deep sub-critical configuration and we have neglected the contributions of precursors. The dominant α-eigenvalue is $\alpha_0 = -0.91112$ (with corresponding k-eigenvalue $k_0 = 0.21945$). The matrix elements

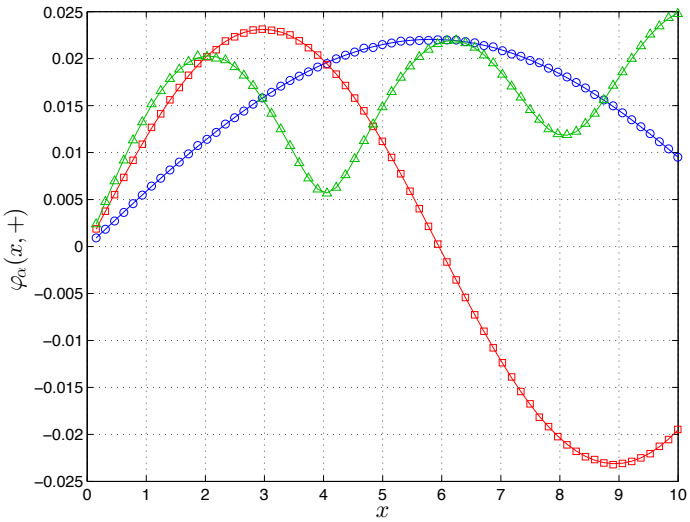

Figure 2: The first few (angular) eigenmodes $\varphi_\alpha(x,+)$: the eigenvectors of the A matrix filled by the Monte Carlo calculation (symbols) are compared to the exact solutions stemming from Eq. (35) (solid lines). Blue circles: fundamental eigenmode $\varphi_{\alpha_0}(x,+)$; red squares: second eigenmode $\varphi_{\alpha_1}(x,+)$; green triangles: third eigenmode $\varphi_{\alpha_2}(x,+)$.

have been computed as described in the previous sections, based on the α-k power iteration. Since the transport model does not depend on energy and only two discrete directions are allowed, the only discretization left is with respect to the space coordinates, which makes easier the investigation of the convergence of the proposed methods.

The Monte Carlo matrix-filling calculation based on the α-k power iteration has been run with 10^3 inactive cycles, 10^3 active cycles used for scoring the matrix elements, and 10^5 particles per cycle. The results of the spectral analysis from the α-weighted matrices are recalled in Tab. 2 for a discretization of $N = 1024$ spatial meshes. An excellent agreement is found between the numerical values coming from the A matrix filled by the Monte Carlo calculation and the exact results stemming from the roots of the dispersion law in Eq. (37). Correspondingly, the first few eigenfunctions are compared in Fig. 2 for the same spatial discretization: again, an excellent agreement is found between the eigenvectors of the A matrix filled by the Monte Carlo calculation and the exact solutions stemming from Eq. (35).

As discussed in the previous sections, an important issue concerns the convergence of the eigenvalues and eigenvectors of A with respect to the size of the

matrix, i.e., the discretization of the viable phase space. The key point is that the use of the α-k power iteration in order to weight the matrix elements by the fundamental φ_α eigenfunction is expected to preserve the fundamental eigenvector of A for any choice of the matrix size. For the purpose of probing the behaviour of A, in addition to the α-weighted matrix we have produced two other matrices obtained by weighting their respective elements by using the fundamental mode of the k-eigenvalue power iteration (with 10^3 inactive cycles, 10^3 active cycles used for scoring the matrix elements, and 10^5 particles per cycle) and by using the flux resulting from a fixed-source calculation starting from a uniformly distributed isotropic source within the domain (with 10^8 particles). In the limit of very large N, all these methods are expected to yield comparable results and to converge to the exact limit $\mathcal{A}$. The corresponding numerical values are recalled in Tab. 2 for $N = 1024$ spatial meshes and different weighting functions.

The convergence analysis of the α eigenvalues as a function of the spatial discretization N and of the choice of the weighting function for A is shown in Fig. 3. As conjectured, the fundamental eigenvalue α_0 resulting from the α-weighted matrix A is unbiased with respect to the exact reference root of the dispersion law in Eq. (37), independently of the discretization N (Fig. 3, left). On the contrary, the fundamental eigenvalues α_0 resulting from the matrix A with the two other weighting schemes shows a bias that is progressively reduced as N increases. Even for this very simple benchmark example, it takes roughly $N = 128$ in order for the other schemes to converge to the true fundamental eigenvalue, which motivates the choice of the α-weighting schemes. Concerning the second and third eigenvalue α_1 and α_2, as expected the higher-order eigenfunctions are not preserved and the α-weighting method does not offer any specific advantage (Fig. 3, right). For higher-order eigenvalues the rate of convergence of the three schemes is similar, and it requires approximatively $N = 256$ to achieve the asymptotic value.

An important issue concerns the impact of the noise intrinsically induced by the Monte Carlo method on the elements of the matrices: in particular, we are interested in assessing the effects of such noise on the derived spectrum and eigenvectors. For this purpose, we have performed an ensemble of independent replicas of the $\alpha - k$ power iterations and we have computed the average and the dispersion of the obtained α spectrum and eigenvectors, as a function of the number of simulated particles per cycle. Numerical findings are reported in Tab. 3 and show that the standard deviation of the first few eigenvalues scales roughly as $1/\sqrt{P}$, P being the number of particles per cycle.

In order to perform a similar analysis on the behaviour of the eigenmodes,

	Particles per cycle	α_0	α_1	$Re[\alpha_{2,3}]$	$Im[\alpha_{2,3}]$
exact		-0.91112104	-1.1402085	-1.5903273	± 0.46007369
Average	10^3	-0.91112119	-1.1449719	-1.6075309	± 0.45378447
	10^4	-0.91112275	-1.1450849	-1.6076210	± 0.45387262
	10^5	-0.91111714	-1.1450994	-1.6076153	± 0.45386983
Std	10^3	2.4×10^{-5}	4.7×10^{-5}	3.3×10^{-5}	6.6×10^{-5}
	10^4	7.6×10^{-5}	1.4×10^{-5}	1.0×10^{-5}	2.0×10^{-5}
	10^5	2.4×10^{-6}	4.7×10^{-5}	3.1×10^{-6}	6.5×10^{-6}

Table 3: Rod model. Comparison of the eigenvalues obtained from the matrices scored during 10^3 replicas of $\alpha - k$ power iterations, each using 10^3 inactive cycles, 10^3 active cycles and a variable number of particles per cycle.

weighting function	R_0	R_1	$R_{2,3}$
exact	0.59054194	3.0407604	1.2570206
$\alpha - k$	0.59067879	3.0393783	1.2640341
k	0.59067531	3.0424330	1.2634575
fixed-source	0.59038753	3.0501619	1.2631744

Table 4: Rod model. Comparison of the firs few estimators R_i obtained from the matrices filled with the method shown in the first column, for $N = 1024$ spatial meshes.

we have introduced an estimator defined as the normalized integral of the i-th eigenfunction over the half-domain, namely,

$$R_i = \frac{|\int_{\frac{L}{2}}^{L} \varphi_{\alpha,i}(x,+)dx|}{|\int_0^L \varphi_{\alpha,i}(x,+)dx|}, \tag{38}$$

where L is the length of the rod. The reference value for R_i can be computed based on Eq. (35). The numerical values for the first few R_i are compared to the exact solutions in Tab. 4 for $N = 1024$ spatial meshes and different weighting functions.

The converge analysis of the estimator R_i estimated by the matrix A as a function of the spatial discretization N and of the choice of the weighting function for A is shown in Fig. 4. As conjectured, the estimator R_0 associated to the fundamental eigenfunction resulting from the α-weighted matrix A is unbiased with respect to the exact solution, independently of the discretization N. On the

	Particles per cycle	R_0	R_1	R_2
exact		0.59054194	3.0407604	1.2570206
average	10^3	0.59049101	3.0517314	1.3023678
	10^4	0.59052498	3.0530707	1.3020484
	10^5	0.59053354	3.0511973	1.3020092
Std	10^3	7.7×10^{-5}	3.3×10^{-3}	2.2×10^{-3}
	10^4	2.4×10^{-5}	1.0×10^{-3}	5.5×10^{-4}
	10^5	7.4×10^{-6}	3.3×10^{-4}	6.2×10^{-5}

Table 5: Rod model. Comparison of the estimators R_i obtained from the matrices scored during 10^3 replicas of $\alpha - k$ power iterations, each using 10^3 inactive cycles, 10^3 active cycles and a variable number of particles per cycle.

contrary, the estimator R_0 resulting from the matrix A with the two other weighting schemes shows a bias that decreases with increasing N. It takes roughly only $N = 8$ in order for the k-weighted scheme to converge to the true fundamental eigenvalue, which can be understood by observing that the deviation between $\varphi_{k,0}(x,+)$ and $\varphi_{\alpha,0}(x,+)$ is rather small for the parameters chosen here. For the matrix weighted on the fixed-source flux, the deviation is much larger, and convergence is achieved after $N = 256$. Concerning the estimators R_1 and R_2 associated with the second and third eigenfunction, all weighting schemes are biased, and the rate of convergence of the three schemes is similar, the asymptotic value being attained after approximatively $N = 128$.

In order to assess the impact of the noise induced by the Monte Carlo method on the eigenvectors, we have performed an ensemble of independent replicas of the $\alpha - k$ power iterations and we have computed the average and the dispersion of the obtained α eigenvectors, as a function of the number of simulated particles per cycle. Numerical findings are reported in Tab. 5 and show that the standard deviation of the first few estimators R_i scales approximately as $1/\sqrt{P}$, P being the number of particles per cycle.

4.1.2. Analysis of the adjoint eigenpairs

We will now focus on the adjoint matrix $A^\dagger$, whose elements have been filled by using the Generalized IFP method, as detailed above. For this example, the Monte Carlo calculation has been performed with 10^8 particles, and 15 latent generations. The α_0 value needed for the Generalized IFP algorithm has been obtained from the direct calculations done in the previous section. The results of the spectral analysis from the adjoint α-weighted matrix are recalled in Tab. 2

Weighting function	$R_0^\dagger$	$R_1^\dagger$	$R_{2,3}^\dagger$
exact	4.0945806×10^{-1}	4.0407604	1.654407
Generalized IFP	4.1054467×10^{-1}	4.0016557	1.6529283
α-k and transposition	4.0981832×10^{-1}	4.0324929	1.6583581

Table 6: Rod model. Comparison of the adjoint estimators $R_i^\dagger$ obtained from the matrices filled with the method shown in the first column, for $N = 1024$ spatial meshes.

for a discretization of $N = 1024$ spatial meshes. An excellent agreement is found between the numerical values coming from the $A^\dagger$ matrix filled by the Monte Carlo calculation and the exact results stemming from the roots of the dispersion law in Eq. (37). This means that the relation $\alpha^\dagger = \alpha$ on the spectrum of the α eigenvalues is correctly preserved when weighting $A^\dagger$ by the fundamental eigenfunction $\varphi_\alpha^\dagger$ [8]. The first few adjoint eigenfunctions are compared in Fig. 5 for the same spatial discretization: again, an excellent agreement is found between the eigenvectors of the $A^\dagger$ matrix filled by the Generalized IFP method and the exact solutions stemming from the eigenfunctions adjoint to Eq. (35). Observe in particular that $\varphi_\alpha^\dagger$ satisfies $\varphi_\alpha^\dagger(x,+) = \varphi_\alpha(x,-)$, as expected.

The convergence of the eigenvalues associated to the $A^\dagger$ matrix is analyzed in Fig. 3: not surprisingly, the convergence of the eigenvalues with respect to the matrix discretization N follows the same pattern as in the direct case. The fundamental eigenvalue α_0 is similarly preserved by the matrix $A^\dagger$, independently of N, whereas the higher eigenvalues are not and converge to the true values in the limit of large N.

In order to analyze the behaviour of the adjoint eigenmodes, we introduce the estimator

$$R_i^\dagger = \frac{|\int_{\frac{L}{2}}^{L} \varphi_{\alpha,i}^\dagger(x,+)dx|}{|\int_0^L \varphi_{\alpha,i}^\dagger(x,+)dx|}. \tag{39}$$

The reference value for $R_i^\dagger$ can be computed based on the adjoint eigenfunctions derived from Eq. (35). Numerical values corresponding to the generalized IFP method and to the transposed matrix obtained from the $\alpha - k$ method are recalled

[8] This property is also preserved when approximating $A^\dagger$ by taking the transposed matrix A^T (although A is weighted by the direct fundamental eigenfunction), since by construction transposition preserves the spectrum.

in Tab. 6 for $N = 1024$ spatial meshes. The converge analysis of the estimator $R_i^\dagger$ estimated by the matrix $A^\dagger$ as a function of the spatial discretization N is shown in Fig. 6. As conjectured, the estimator $R_0^\dagger$ associated to the fundamental adjoint eigenfunction resulting from the adjoint α-weighted matrix $A^\dagger$ is unbiased with respect to the exact solution, independently of the discretization N. As for the estimator $R_1^\dagger$ associated with the second eigenfunction, the adjoint α-weighted matrix $A^\dagger$ yields a biased result, which converges to the exact limit after approximatively $N = 32$.

In the same figure we also display the estimators of the adjoint eigenfunctions obtained by taking the transposed direct α-weighted matrix A^T in order to approximate $A^\dagger$. Figure 6 shows that this approach leads to a bias on $R_i^\dagger$ for the fundamental and the first eigenfunction. Although the bias vanishes as expected in the limit of large N, this analysis suggests that it is general preferable to compute $A^\dagger$ rather than approximating the adjoint-weighted matrix by using the transposed matrix A^T.

4.2. A continuous-energy transport model

We consider now a continuous-energy transport model in an infinite medium. The model includes scattering with an amnesia kernel (Duderstadt and Martin, 1979), capture and fission with two precursor families. All cross sections Σ_r are assumed to have a $1/\sqrt{E}$ behaviour, i.e., $\Sigma_r(E) = \Sigma_r^0/\sqrt{E}$. The scattering kernel $M(E)$ is a Maxwell distribution [9] with average energy E_s. The prompt $\chi_p(E)$ and delayed $\chi_{d,j}(E)$ fission kernels are also assumed to be Maxwellian distributions with average E_p and $E_{d,j}$, $j = 1,2$, respectively. The fission multiplicities are taken constant, for the sake of simplicity. The resulting α eigenvalue problem reads

$$\left[\frac{\alpha}{v(E)} + \Sigma_t(E)\right]\varphi_\alpha(E) = M(E)\int dE'\Sigma_s(E')\varphi_\alpha(E') + \chi_p(E)\int dE'\nu_p\Sigma_f(E')\varphi_\alpha(E') + \sum_j \frac{\lambda_j}{\lambda_j+\alpha}\chi_{d,j}(E)\int dE'\nu_{d,j}\Sigma_f(E')\varphi_\alpha(E'), \quad (41)$$

[9] The normalized Maxwell probability density $\mathcal{M}(x)$ is given by

$$\mathcal{M}(x) = \frac{2}{\sqrt{\pi}}\frac{1}{\theta^{3/2}}\sqrt{x}e^{-x/\theta}, \quad (40)$$

where θ is the average of the distribution.

where $v(E) = \sqrt{E}$. By virtue of the simple functional forms chosen for this configuration, the eigenvalues and eigenfunctions can be determined exactly. In particular, the eigenvalues are the roots of the dispersion law

$$\Lambda(\alpha) = \alpha + \Sigma_a^0 - \nu_p \Sigma_f^0 - \sum_j \frac{\lambda_j}{\lambda_j + \alpha} \nu_{d,j} \Sigma_f^0 = 0, \tag{42}$$

where $\Sigma_a^0 = \Sigma_t^0 - \Sigma_s^0$, and the eigenfunctions read

$$\varphi_\alpha(E) = \frac{\sqrt{E}}{\alpha + \Sigma_t^0} \left[\Sigma_s^0 M(E) + \nu_p \Sigma_f^0 \chi_p(E) + \sum_j \frac{\lambda_j}{\lambda_j + \alpha} \nu_{d,j} \Sigma_f^0 \chi_{d,j}(E) \right], \tag{43}$$

for the values α that satisfy the dispersion law. As for the adjoint eigenvalue problem, we have the equation

$$\begin{aligned} \left[\frac{\alpha}{v(E)} + \Sigma_t(E) \right] \varphi_\alpha^\dagger(E) = \Sigma_s(E) \int dE' M(E') \varphi_\alpha^\dagger(E') + \nu_p \Sigma_f(E) \int dE' \chi_p(E') \varphi_\alpha^\dagger(E') \\ + \sum_j \frac{\lambda_j}{\lambda_j + \alpha} \nu_{d,j} \Sigma_f(E') \int dE' \chi_{d,j}(E') \varphi_\alpha^\dagger(E'). \end{aligned} \tag{44}$$

By inspection, the eigenfunctions are $\varphi_\alpha^\dagger(E) = 1$, independently of α, with the same associated spectrum as in the direct problem.

For this example, we have chosen the following parameters: $\Sigma_c^0 = 0.6$, $\Sigma_s^0 = 0.3$, $\Sigma_f^0 = 0.1$; for the fission multiplicities we have set $\nu_p = 2$ and $\nu_{d,j} = \beta_j \nu_d$, with $\nu_d = 0.5$, $\beta_1 = 0.25$ and $\beta_2 = 0.75$; for the scattering law we have taken $E_s = 10^{-5}$; for the prompt and delayed fission kernels we have taken the averages $E_p = 1$, $E_{d,1} = 0.1$ and $E_{d,2} = 0.01$, respectively; for the precursor decay constants we have taken $\lambda_1 = 2.5$ and $\lambda_2 = 5$.

The first few eigenvalues obtained from the matrices are compared to the reference solutions in Tab. 7 for $N = 1024$ energy meshes. The direct eigenfunctions resulting from the matrices filled by α-k power iteration (with 10^3 inactive cycles, 10^3 active cycles and 10^5 particles per cycle) are compared to the analytical solutions in Fig. 7, for a discretization corresponding to $G = 256$ energy intervals. The first few modes are in excellent agreement with the reference solutions. The numerical findings for the adjoint problem, obtained from the Generalized IFP method with 10^8 particles and 15 latent generations, are shown in Fig. 8: again, an excellent agreement is found between the eigenvectors stemming from the matrices and the exact solutions, despite the fact that the adjoint eigenfunctions for this problem are degenerate.

weighting function	α_0	α_1	α_2
exact	-0.44365178	-2.5149493	-5.0413989
α-k	-0.4436851	-2.5149039	-5.0414104
Generalized IFP	-0.443671223	-2.5149282	-5.0413210

Table 7: Continuous-energy model. Comparison of the first few eigenvalues obtained from the matrices scored with the method shown in the first column, with $N = 1024$ energy groups.

5. Discussion

The examples discussed in the previous section are very simple and have been precisely chosen in order to compare the obtained numerical results against reference solutions. In view of the application of the proposed methods to real-world reactor configurations, some issues must be carefully examined and taken into account.

The first concerns the size of the matrix operators and hence the involved memory footprint. A first glance to the involved order of magnitudes might suggest that the overall size of the matrices involved in α-eigenvalue problems may become too large to work with for any practical case, due to the need of separately discretizing space, direction and energy (contrary to the k-eigenvalue problem, where only a spatial discretization is typically required (Dufek and Gudowski, 2009; Carney et al., 2014)). Consider for instance a three-dimensional configuration, and assume that each variable is partitioned into 10^2 bins: this would lead to a total number of 10^{10} bins, i.e., to a number of 10^{20} matrix entries. This applies to both direct and adjoint matrices. Such huge number clearly corresponds to an unaffordable memory footprint [10] on current machines (and on future, at least for a very long time).

In practice, however, the α-eigenvalue matrices have been already applied to realistic systems, including small research reactors (Betzler, 2014; Betzler et al., 2018): as discussed in Sec. 3, the involved matrices have a sparse nature, and the number of non-null entries is much smaller that the total size of the matrices (see in particular Eq. (24)). Furthermore, one can often take advantage of the existing symmetries in order to reduce the dimension of the problem. Moreover, for the energy and angle variable 10^2 bins are probably excessive with respect to most problems of interest. To provide an example, for a two-dimensional

[10] Suppose that each entry is represented by a double-precision floating-point number.

representation of a reactor core, by taking $Nx = N_y = 10^2$ for the spatial mesh, $M = 8$ for the directions, $G = 30$ for the energy groups and $J = 6$ for the precursor families, we would have $\sim 6\times10^{13}$ bins for the full matrix, but less than $\sim 6\times10^{8}$ non-null entries. Even in this case, however, and despite all the simplifications, the memory footprint would be challenging for current machines. Numerical tests of convergence should be also performed a posteriori in order to ensure that at least the spatial shape of the eigenvectors has been correctly captured. The benchmark configurations examined in this manuscript clearly do not address these problems, since only a single dimension has been discretized and careful convergence tests were thus possible.

The second issue concerns the applicability of these matrices to the analysis of system changes. The whole α-eigenvalue expansion is based on the assumption that the physical properties of the system under analysis (such as cross sections, fission spectra, multiplicities, etc.) do not evolve with time: eigenvalues and eigenvectors are computed for a specific state. In real-world configurations, these properties naturally change, due to external actions (control rod movements), physical feedbacks (Doppler effect, etc.), or both. In principle, once the system changes the computed alpha eigenvalues and eigenvectors are no longer valid and cannot be used. This leads to two different approaches: one can either introduce (short) time steps and re-compute the required matrices at each time step, or use some clever interpolation between the initial and final configurations of the system. The former method would lead to an unreasonable memory occupation (and most probably also computation time). The latter method has been suggested (Laureau et al., 2015) and successfully applied (Laureau et al., 2017b) for the Transient Fission Matrix approach, and seems thus much more promising [11].

In view of these considerations, and based on the increasing availability of direct time-dependent Monte Carlo simulations for reactor physics problems (which natively include moving geometries and physical feedbacks (Sjenitzer and Hoogenboom, 2013; Faucher et al., 2018)), the main interest of the α-eigenvalue matrix operators seems for higher-order mode analysis rather than for reconstructing the time evolution of a system via eigenmode expansion: knowledge of the first few α-eigenvalues and eigenfunctions for a given reactor state might help, e.g., in locating the most appropriate detector positions for on-line core monitoring. Nonetheless, a comparison in terms of performances and accu-

[11] In particular, the application of perturbation techniques such as correlated sampling has been shown to enhance the performances of the interpolation methods in realistic applications, including multi-physics feedbacks (Laureau et al., 2017a).

racy with respect to existing matrix-based methods (using time-dependent Monte Carlo methods as a reference) for the approximation of the reactor kinetics will deserve further investigation.

6. Conclusions

Knowledge of the α eigenpairs is key to several applications in reactor physics. In a series of recent works, it has been proposed to use Monte Carlo methods in order to estimate the elements of the matrices that represent the discretized formulation of the operators involved in the α-eigenvalue problem. In this work, we have suggested some strategies to overcome two possible shortcomings of the existing algorithms. We have shown that the bias possibly appearing on the direct fundamental eigenvalue and eigenvector for smaller sizes of the discretized matrix can be removed by using the α-k modified power iteration method as a weighing function. This corresponds to weighting the matrix elements by the fundamental mode φ_α, which is expected to preserve the fundamental eigenvalue and eigenvector of the matrix, similarly to what occurs for the fission matrix in k-eigenvalue problems. We have successively shown that the matrix associated to the adjoint α-eigenvalue problem can be estimated by using the Generalized Iterated Fission Probability method, which was recently introduced as a reference Monte Carlo method to compute the fundamental adjoint α eigenfunction. Since this approach corresponds to weighting the matrix elements by the fundamental adjoint eigenfunction, the fundamental adjoint eigenvector of the discretized matrix will be similarly preserved.

The proposed direct and adjoint methods have been verified on two benchmark problems where exact reference solutions were available for both the eigenvalue spectrum and the direct and adjoint eigenfunctions, and their convergence and accuracy have been extensively assessed. The impact of alternative weighting schemes (such as the k-eigenvalue fundamental mode or the flux resulting from solving a fixed-source problem) and the differences between the adjoint matrix and the transposed direct matrix are most probably emphasized by the choice of the benchmark problems presented in this paper: future work will be aimed at extensively assessing the performances and the robustness of the proposed method for more realistic configurations combining spatial and energy heterogeneities.

We conclude by observing that the strategy presented in this paper in order to fill the matrix elements of the adjoint matrix by the Generalized IFP method might be easily extended to the k-eigenvalue formulation: instead of using the transposed direct fission matrix, one could use the regular IFP method (which

yields the importance function for the k-eigenvalue problems) so as to produce the adjoint fission matrix, thus avoiding the bias on the fundamental adjoint eigenvector.

Acknowledgements

The authors wish to thank Dr. F. Malvagi (CEA/Saclay) for many fruitful discussions.

G. Bell and S. Glasstone. *Nuclear Reactor Theory*. Van Nordstrand Reinhold Company, 1970.

B. R. Betzler. *Calculating Alpha Eigenvalues and Eigenfunctions with a Markov Transition Rate Matrix Monte Carlo Method*. PhD thesis, University of Michigan, 2014.

B. R. Betzler, W. R. Martin, B. C. Kiedrowski, and F. B. Brown. Calculating Alpha Eigenvalues of One-Dimensional Media with Monte Carlo. *Journal of Computational and Theoretical Transport*, 43:3849, 2014.

B. R. Betzler, B. C. Kiedrowski, F. B. Brown, and W. R. Martin. Calculating Infinite-medium Alpha-eigenvalue Spectra with Monte Carlo using a Transition Rate Matrix Method. *Nuclear Engineering and Design*, 295:639644, 2015.

B. R. Betzler, B. C. Kiedrowski, W. R. Martin, and F. B. Brown. Calculating Alpha Eigenvalues and Eigenfunctions with a Markov Transition Rate Matrix Monte Carlo Method. *Nuclear Science and Engineering*, 192:115152, 2018.

D. Brockway, P. Soran, and P. Whalen. Monte Carlo alpha calculations. Technical Report LA-UR-85-1224, Los Alamos National Laboratory, 1985.

Y. Cao and J. C. Lee. Spatial corrections for pulsed-neutron reactivity measurements. *Nuclear Science and Engineering*, 165(3):270–282, 2010.

S. Carney, F. Brown, B. Kiedrowski, and W. Martin. Theory and applications of the ssion matrix method for continuous-energy Monte Carlo. *Annals of Nuclear Energy*, 73:423–431, 2014.

D. Cullen. Static and dynamic criticality: are they different? Technical Report UCRL-TR-201506, University of California Radiation Laboratory, 2003.

J. Duderstadt and W. Martin. *Transport theory*. J. Wiley and sons, New York, 1979.

J. Dufek and W. Gudowski. Fission matrix based Monte Carlo criticality calculations. *Annals of Nuclear Energy*, 36:1270–1275, 2009.

M. Faucher, D. Mancusi, and A. Zoia. New kinetic simulation capabilities for Tripoli-4: methods and applications. *Annals of Nuclear Energy*, 120:74–88, 2018.

J. A. Favorite. SENSMG: First-Order Sensitivities of Neutron Reaction Rates, Reaction-Rate Ratios, Leakage, keff, and α Using PARTISN. *Nuclear Science and Engineering*, 192(1): 80–114, 2018.

D. S. Grebenkov and B. T. Nguyen. Geometrical structure of Laplacian eigenfunctions. *SIAM Review*, 55:601–667, 2013.

G. Hansen. Rossi alpha method. Technical Report LA-UR-85-4176, Los Alamos National Laboratory, 1985.

T. Hill. Efficient methods for time absorption (alpha) eigenvalue calculations. Technical Report LA-9602-MS (UC-32), Los Alamos National Laboratory, 1983.

J. Hoogenboom. Numerical calculation of the delayed-alpha eigenvalue using a standard criticality code. In *Physor 2002*, Seoul, Korea, 2002.

A. Jinaphanh and A. Zoia. Perturbation and sensitivity calculations for time eigenvalues using the generalized iterated fission probability. *Annals of Nuclear Energy*, 133:678–687, 2019.

C. Josey and F. B. Brown. Computing alpha eigenvalues using the fission matrix. In *M&C2019*, Portland, Oregon, USA, 25-29 August 2019.

C. J. Josey. General Improvements to the MCNP Alpha-Eigenvalue Solver. Technical Report LA-UR-18-22738, Los Alamos National Laboratory, 2018.

H. G. Kaper. The initial-value transport problem for monoenergetic neutrons in an infinite slab with delayed neutron production. *Journal of Mathematical Analysis and Applications*, 19: 207–230, 1967.

G. Keepin. *Physics of Nuclear Kinetics*. Addison-Wesley, Reading, UK, 1965.

B. C. Kiedrowski, F. B. Brown, and P. P. H. Wilson. Adjoint-Weighted Tallies for k-Eigenvalue Calculations with Continuous-Energy Monte Carlo. *Nuclear Science and Engineering*, 168 (3):226–241, 2011.

E. Larsen and P. F. Zweifel. On the spectrum of the linear transport operator. *Journal of Mathematical Physics*, 15:1987–1997, 1974.

A. Laureau, M. Aufiero, P. Rubiolo, E. Merle-Lucotte, and D. Heuer. Transient fission matrix: kinetic calculation and kinetic parameters β_{eff} and λ_{eff} calculation. *Annals of Nuclear Energy*, 85:1035 – 1044, 2015.

A. Laureau, L. Buiron, B. Fontaine, and V. Pascal. Fission matrix interpolation for the tfm approach based on a local correlated sampling technique for fast spectrum heterogeneous reactors. In *M&C2017*, Jeju, Korea, 16-20 April 2017a.

A. Laureau, D. Heuer, E. Merle-Lucotte, P. Rubiolo, M. Allibert, and M. Aufiero. Transient coupled calculations of the molten salt reactor using the transient fission matrix approach. *Nuclear Engineerign and Design*, 316:112 – 124, 2017b.

D. Mancusi and A. Zoia. Chaos in eigenvalue search methods. *Annals of Nuclear Energy*, 112: 354 – 363, 2018.

B. Montagnini and V. Pierpaoli. The time-dependent rectilinear transport equation. *Transport Theory and Statistical Physics*, 1:59–75, 1971.

Y. Nauchi. Attempt to estimate reactor period by natural mode eigenvalue calculation. In *Proceedings of SNA+MC 2013*, Paris, France, 2013.

Y. Nauchi and T. Kameyama. Development of Calculation Technique for Iterated Fission Probability and Reactor Kinetic Parameters Using Continuous-Energy Monte Carlo Method. *Journal of Nuclear Science and Technology*, 47:977–990, 2010.

I. Pázsit and L. Pál. *Neutron Fluctuations: A Treatise on the Physics of Branching Processes*. Elsevier, Oxford, UK, 2008.

C. Persson. Pulsed neutron source measurements in the subcritical ADS experiment YALINA-Booster. *Annals of Nuclear Energy*, 35:2357–2364, 2008.

W. Pfeiffer, J. Brown, and A. Marshall. Fort St. Vrain startup test A-3: Pulsed-Neutron experiments. Technical Report GA-A13079, General Atomic, 1974.

R. Sanchez and P. Jaegers. Prompt neutron decay constants and subcritical measurements for material control and accountability in SHEBA. In *International conference on the physics of nuclear science and technology*, Long Island, New York, United States, 5-8 October 1998.

H. J. Shim, S. H. Jang, and S. M. Kang. Monte carlo alpha iteration algorithm for a subcritical system analysis. *Science and Technology of Nuclear Installations*, 2015:859242 (7 pages), 2015.

B. L. Sjenitzer and J. E. Hoogenboom. Dynamic Monte Carlo Method for Nuclear Reactor

Kinetics Calculations. *Nuclear Science and Engineering*, 175:94–107, 2013.

N. Terranova, D. Mancusi, and A. Zoia. Generalized Iterated Fission Probability for Monte Carlo eigenvalue calculations. *Annals of Nuclear Energy*, 108:57–66, 2017.

I. Variansyah, B. R. Betzler, and W. R. Martin. Alpha-weighted transition rate matrix method. In *M&C2019*, Portland, Oregon, USA, 25-29 August 2019.

G. Wing. *An introduction to transport theory*. Wiley and sons, New York, 1962.

T. Yamamoto. Higher order alpha mode eigenvalue calculation by Monte Carlo power iteration. *Progress in Nuclear Science and Technology*, 2:826–835, 2011.

T. Yamamoto and H. Sakamoto. A Monte Carlo technique for sensitivity analysis of alpha-eigenvalue with the differential operator sampling method. *Annals of Nuclear Energy*, 127: 178–187, 2019.

A. Zoia and E. Brun. Reactor physics analysis of the spert iii e-core with TRIPOLI-4® . *Annals of Nuclear Energy*, 90:71 – 82, 2016.

A. Zoia, E. Dumonteil, and A. Mazzolo. Properties of branching exponential flights in bounded domains. *EPL*, 100:40002, 2012.

A. Zoia, E. Brun, and F. Malvagi. Alpha eigenvalue calculations with TRIPOLI-4® . *Annals of Nuclear Energy*, 63:276 – 284, 2014.

A. Zoia, E. Brun, F. Damian, and F. Malvagi. Monte Carlo methods for reactor period calculations. *Annals of Nuclear Energy*, 75:627 – 634, 2015.

A. Zoia, Y. Nauchi, E. Brun, and C. Jouanne. Monte carlo analysis of the crocus benchmark on kinetics parameters calculation. *Annals of Nuclear Energy*, 96:377 – 388, 2016.

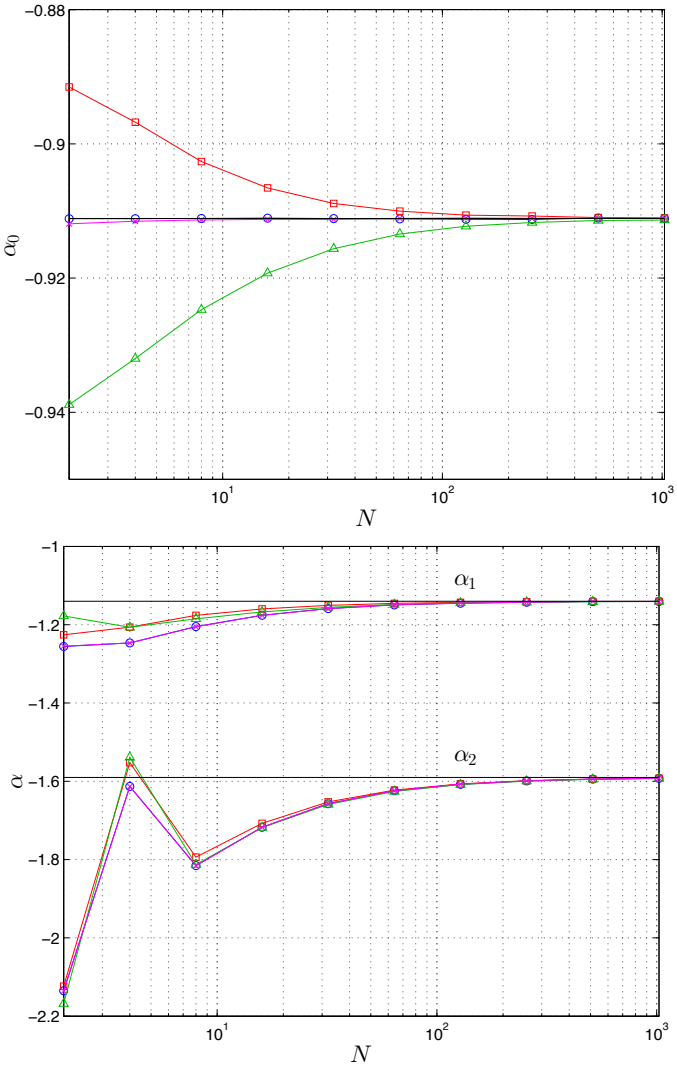

Figure 3: Convergence of the first few eigenvalues α_i as a function of the number of spatial meshes N and of the weighting function for the matrix A. Left: the fundamental eigenvalue α_0; right: α_1 and α_2. Black solid lines correspond to the exact reference values from the roots of the dispersion law in Eq. (37). Blue circles correspond to results obtained from the α-weighted A matrix; red squares to the k-weighted A matrix; green triangles symbols to the matrix A weighted by a fixed-source flux. Solid lines have been added to guide the eye. In addition, we display with magenta diamonds the corresponding eigenvalues obtained from the adjoint matrix $A^\dagger$ weighted by the adjoint α-eigenfunction resulting from the Generalized IFP method.

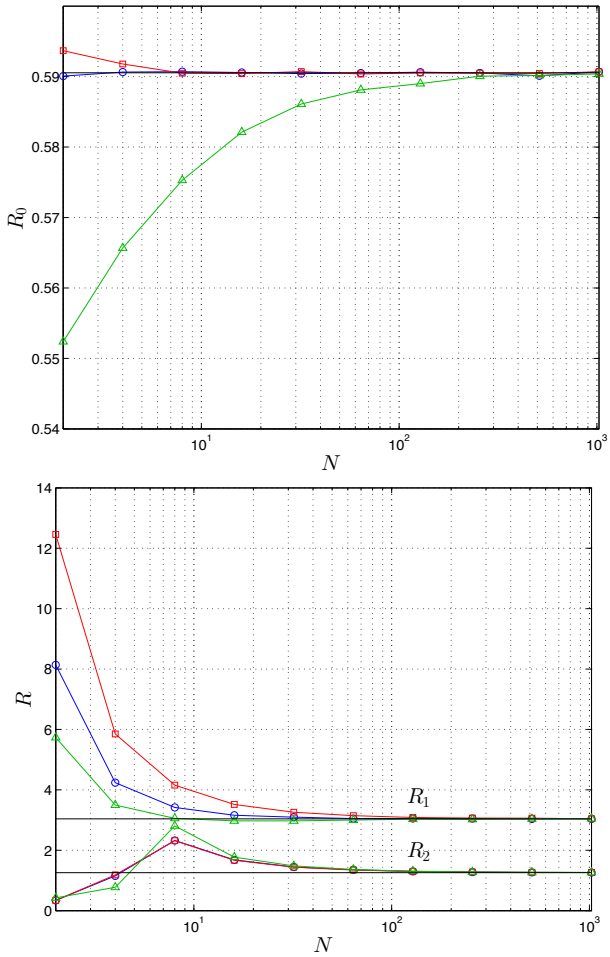

Figure 4: Convergence of the first few estimators R_i as a function of the number of spatial meshes N and of the weighting function for the matrix A. Black solid lines correspond to the exact reference values based on Eq. (35). Blue circles correspond to results obtained from the α-weighted A matrix; red squares correspond to the k-weighted A matrix; green triangles correspond to the matrix A weighted by a fixed-source flux. Left: the estimator R_0 associated to the fundamental eigenfunction $\varphi_{\alpha,0}(x,+)$; right: the estimator R_1 associated to the second eigenfunction $\varphi_{\alpha,1}(x,+)$ and the estimator R_2 associated to the second eigenfunction $\varphi_{\alpha,2}(x,+)$. Solid lines have been added to guide the eye.

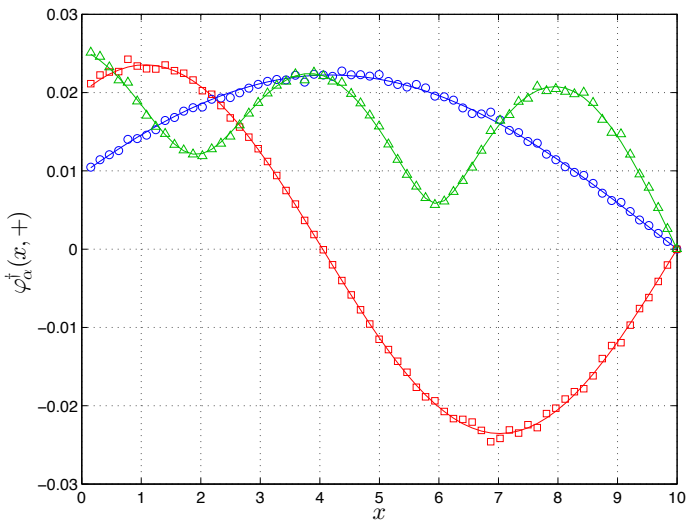

Figure 5: The first few (angular) adjoint eigenmodes $\varphi_\alpha^\dagger(x,+)$: the eigenvectors of the A matrix filled by the Monte Carlo calculation (symbols) are compared to the exact solutions stemming from the equation adjoint to Eq. (35) (solid lines). Blue circles: fundamental adjoint eigenmode $\varphi_{\alpha_0}^\dagger(x,+)$; red squares: second adjoint eigenmode $\varphi_{\alpha_1}^\dagger(x,+)$; green triangles: third adjoint eigenmode $\varphi_{\alpha_2}^\dagger(x,+)$.

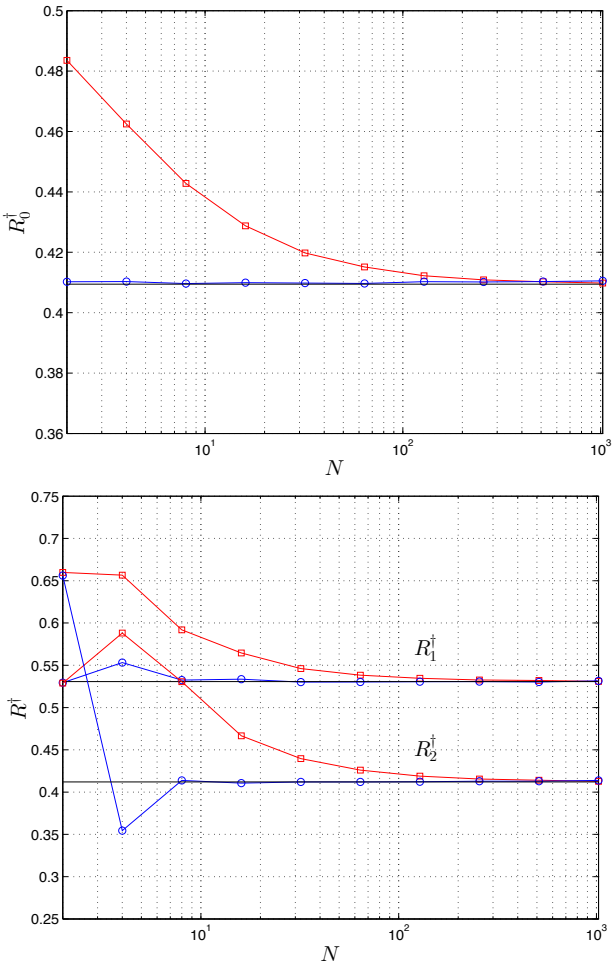

Figure 6: Convergence of the first few estimators $R_i^\dagger$ as a function of the number of spatial meshes N. Black solid lines correspond to the exact reference values based on Eq. (35). Blue circles correspond to results obtained from the adjoint α-weighted $A^\dagger$ matrix; red squares correspond to the direct α-weighted A^T matrix. Left: the estimator $R_0^\dagger$ associated to the fundamental adjoint eigenfunction $\varphi_{\alpha,0}^\dagger(x,+)$; right: the estimator $R_1^\dagger$ associated to the second adjoint eigenfunction $\varphi_{\alpha,1}^\dagger(x,+)$ and the estimator $R_2^\dagger$ associated to the second adjoint eigenfunction $\varphi_{\alpha,2}^\dagger(x,+)$. Solid lines have been added to guide the eye.

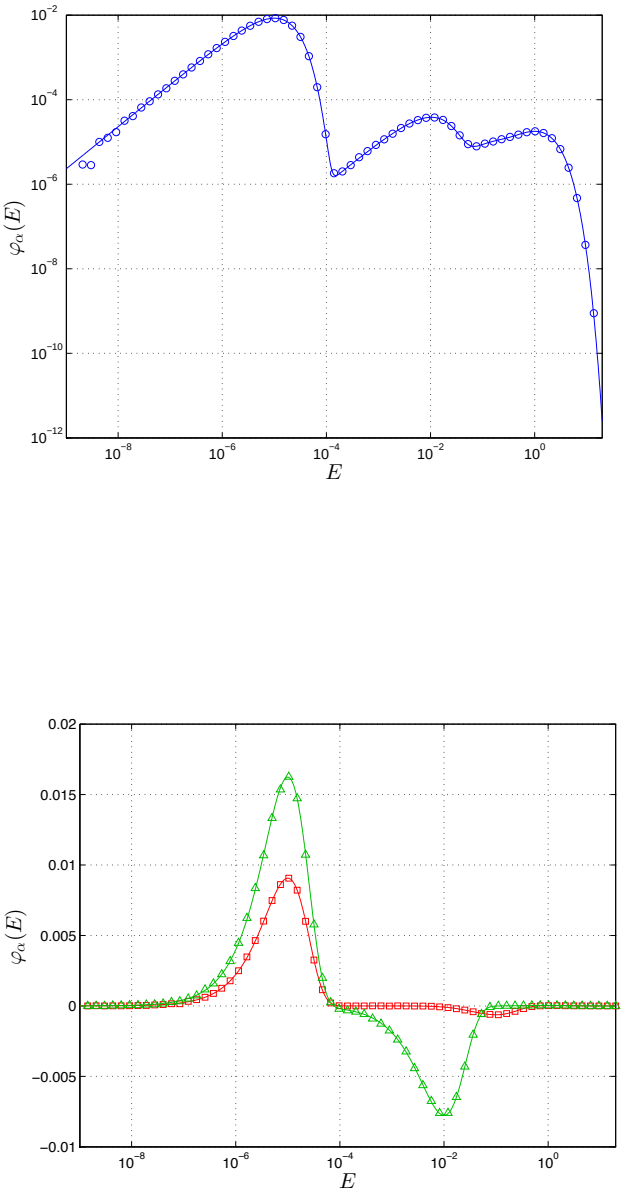

Figure 7: A continuous-energy transport problem. Comparison of the direct eigenfunctions resulting from the matrices filled by α-k power iteration (displayed as symbols) with the reference solutions given in Eq. 43 (displayed as solid lines). Left: blue circles denote the fundamental eigenfunction $\varphi_{\alpha_0}(E)$: right: red squares the second eigenfunction $\varphi_{\alpha_1}(E)$ and green triangles the third eigenfunction $\varphi_{\alpha_2}(E)$.

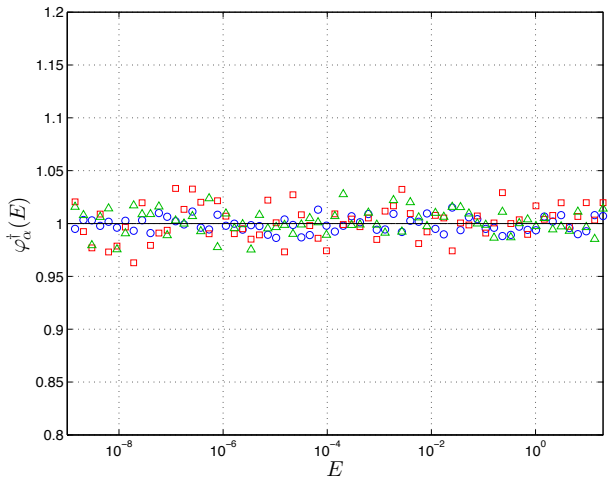

Figure 8: A continuous-energy transport problem. Comparison of the adjoint eigenfunctions resulting from the matrices filled by Generalized IFP method (displayed as symbols) with the reference solutions given in Eq. 43 (displayed as solid lines). Blue circles denote the fundamental adjoint eigenfunction $\varphi^{\dagger}_{\alpha_0}(E)$; red squares the second adjoint eigenfunction $\varphi^{\dagger}_{\alpha_1}(E)$; green triangles the third adjoint eigenfunction $\varphi^{\dagger}_{\alpha_2}(E)$.